LC-PHSM-2007-001

Simulation of the measurement of the hadronic branching ratios for a light Higgs boson at the ILC

Thorsten Kuhl
Institut für Physik, Universität Mainz
Stuadingerweg 7, D-55099 Mainz, Germany

Klaus Desch
Physikalisches Institut der Universität Bonn
Nussallee 12, D-53115 Bonn, Germany

Abstract

A simulation and analysis for the measurement of the Higgs Boson branching ratios BR(H→ $b\bar{b}$), BR(H→ $c\bar{c}$) and BR(H→ gg) for a Standard Model like light Higgs boson ($m_H = 120\,\mathrm{GeV}$) at the International Linear Collider (ILC) is presented. The analysis is performed at a centre-of-mass energy of $\sqrt{s} = 350\,\mathrm{GeV}$ and for an integrated luminosity of $500\,\mathrm{fb}^{-1}$. Only the Higgs-strahlung process is taken as the signal process. After the event selection a simultaneous fit of the branching ratios is applied. The relative statistical errors obtained for the measurement of $\sigma\times$ BR(H→X) are 1.0% (X= $b\bar{b}$), 12.3% (X= $c\bar{c}$), and 8.3% (X= gg). For $m_H = 140\,\mathrm{GeV}$ and an integrated luminosity of $1\,\mathrm{ab}^{-1}$, the relative errors are 1.8% (X= $b\bar{b}$), 27% (X= $c\bar{c}$), and 16% (X= gg). The results are compared to previous studies.

1 Introduction

During the past years many simulations have been performed to investigate the prospects for measuring Higgs boson properties at a future Linear Collider [1, 2, 3]. Precission electroweak data interpreted within the Standard Model (SM) favour a light Higgs boson. The precise measurement of the Higgs boson branching fractions at the ILC is a crucial test both for the Higgs mechanism itself and in order to distinguish the SM from extensions.

In this note the Higgs boson mass is assumed to be $m_H = 120\,\mathrm{GeV}$. For this mass the dominant Higgs boson decays are into pairs of bottom and charm quarks and gluons. In addition, a slightly modified selection was applied to a Higgs boson mass of $m_H = 140\,\mathrm{GeV}$, where the decay into pairs of W-Bosons becomes important.
Since the publication of the TESLA technical design report (TDR [1]), many improvements have been achieved in the simulation of vertex reconstruction for the fast parametric simulation program SIMDET [4]. For the first time, a track-wise vertex finding and flavour tagging algorithm is used while previously only a coarse parametrisation was available.

2 Event generation and data samples

The signal process consists of Higgs bosons produced in Higgsstrahlung, $e^+e^- \rightarrow HZ$, and decaying into pairs of bottom or charm quarks or gluons The signal process consists of Higgs bosons produced in Higgs decays into other decay channels, in particular W^+W^- and Z^0Z^0 and $\tau^+\tau^-$, as well as Higgs bosons produced through the W^+W^-/Z^0Z^0 fusion processes, $e^+e^- \rightarrow H\nu\bar{\nu}/e^+e^-$ are considered as backgrounds in this analysis.

Signal and dominant background events are generated with PYTHIA6.2 [5]. Cross sections are also taken from PYTHIA. For the simulation of beamstrahlung the CIRCE package [6] is used. SM Higgs boson branching fractions are calculated with HDECAY [8] as listed in Table 1. Around 75000 events from Higgs-strahlung are expected for a $m_H = 120\,\mathrm{GeV}$ and an integrated luminosity of $500\,\mathrm{fb}^{-1}$. The background cross sections and the numbers of generated background events are listed in Table 2. The dominant SM 2-fermion and resonant 4-fermion processes with at least one quark pair in the final state are taken into account. Background from two-photon processes is found to be negligible. Altogether, 3.5×10^7 background events from the considered processes are expected for a luminosity of $500\,\mathrm{fb}^{-1}$. In order to be largely independent of statistical fluctuations in the extraction of the branching ratios, $5\,\mathrm{ab}^{-1}$ of signal and background events are simulated.

	SM Higgs branching ratio (in %)	
Decay mode	$m_H = 120\,\mathrm{GeV}$	$m_H = 140\,\mathrm{GeV}$
$b\bar{b}$	68.16	34.11
$c\bar{c}$	3.04	1.52
gg	6.71	4.68
$\tau^+\tau^-$	6.74	3.47
W^+W^-	13.45	49.03
Z^0Z^0	1.48	6.70

Table 1: *SM Higgs boson branching ratios for the major decay modes calculated with HDECAY [8].*

For the simulation of the detector response, SIMDET3 [4], a fast parametric cluster and track smearing program, is used. The parameterised detector is based on the TESLA technical design report [1]. Relevant resolution parameters are extracted from the full GEANT3-based simulation BRAHMS [9]. In contrast to previous versions of SIMDET, the simulation of the track parameters for charged particles originating from the decay of long-lived particles is improved.

Process	Cross section (pb)	Generated events
$e^+e^- \rightarrow Z^0/\gamma* \rightarrow q\bar{q}(\gamma)$	27.28	1.4×10^8
$e^+e^- \rightarrow W^+W^- \rightarrow q\bar{q}q\bar{q}$	6.10	3×10^7
$e^+e^- \rightarrow W^+W^- \rightarrow q\bar{q}l\nu$	5.85	3×10^7
$e^+e^- \rightarrow Z^0Z^0 \rightarrow q\bar{q}q\bar{q}$	0.48	4×10^6
$e^+e^- \rightarrow Z^0Z^0 \rightarrow q\bar{q}l^+l^-$	0.20	2×10^6
$e^+e^- \rightarrow Z^0Z^0 \rightarrow q\bar{q}\nu\bar{\nu}$	0.24	2×10^6
$e^+e^- \rightarrow We\nu \rightarrow q\bar{q}e\bar{\nu}$	2.48	1.2×10^7
$e^+e^- \rightarrow Z^0e^+e^- \rightarrow q\bar{q}e^+e^-$	13.33	7×10^7

Table 2: *Production cross section and generated numbers of events for the dominant SM background processes at* $\sqrt{s} = 350\,\mathrm{GeV}$ *calculated with PYTHIA [5].*

3 Tools

The identification of leptons, photons and jets is an important part of the analysis. For the jets a flavour tagging tool based on ZVTOP [10] algorithm is used to estimate the primary quark content. Afterwards a kinematic fit is useful to improve the reconstruction of jet energies and directions. In this section the most important reconstruction tools are shortly described.

3.1 Photon and Lepton Identification

Photons from initial state radiation occur much more often in the background than in the signal, where the phase space photon radiation is smaller. Lepton identification is important for the selection of leptonic Z decays and for the rejection of semileptonic W-decays.

Instead of the parameterised photon and lepton identification implemented in SIMDET an analysis based on tracking and calorimeter information is used [12].

3.1.1 Photon selection

Photons from initial state radiation and beamstrahlung are produced independent of the main process. Most times these photons are well separated from tracks. High energetic well isolated neutral energy depositions are selected as photons. A photon has to satisfy the following conditions:

- a calorimeter cluster with energy exceeding 5 GeV;
- no charged particle track within a cone of 15 deg around the cluster position;
- less that 15% of the cluster energy deposited in the hadronic calorimeter.

In further analysis steps, all photons are collected and the centre-of-mass system is corrected assuming that all photons are coming from initial state radiation. Events with a sum of photonic energy larger than 100 GeV are rejected.

3.1.2 Electron and muon identification

In the case the Z Boson decays into a lepton pair, it is very helpful to identify the leptons before the reconstruction of the remaining event. Additional single electrons and muons can be used to veto semileptonic W decays.

An electron is reconstructed as high energetic isolated track with an associated cluster in the electromagnetic calorimeter and vanishing energy in the hadronic calorimeter. It has to satisfy:

- a charged particle track with momentum larger than 4 GeV associated with a calorimeter cluster;
- no further track within 5 deg;
- the energy of the associated cluster in the hadronic calorimeter has to be less than 2 GeV and less than 5% of the cluster energy in the hadronic calorimeter.

Muons are identified as minimum ionising particles:

- a charged particle track with a momentum larger than 4 GeV;
- no further track within 5 deg;
- the energy of the associated cluster has to be consistent with the expectation for a minimum ionising particle, i.e. ≈ 1.2 GeV in the electromagnetic calorimeter and ≈ 2.6 GeV in the hadronic calorimeter.

3.2 Jets and jet flavour reconstruction

At linear collider energies the fragmentation products of primary partons, quarks and gluons, produce collimated jets. Jets are reconstructed from particle flow objects, i.e. tracks and unassociated clusters, with the DURHAM jet algorithm [13]. Afterwards, a kinematic fit is applied to improve the jet energy and angular resolution. The flavour of the jets is reconstructed using a flavour tagging neural net based on ZVTOP [10].

3.2.1 Jet finding

For the identification of the primary partons the fragmentation products of the hadronic systems are forced into jets. In this note the DURHAM or k_T algorithm [13] is used to force the corresponding particle flow objects into two (for $Z \rightarrow \nu\nu, l\bar{l}$) or four jets (for $Z \rightarrow q\overline{q}$) (see Section 4.1).

3.2.2 Kinematic Fits

In the hadronic ($Z \rightarrow q\overline{q}$) and leptonic ($Z \rightarrow \ell^+\ell^-$) channels, all four primary partons are reconstructed. In this case a kinematic fit with 5 constraints (5C) was applied to optimise the Higgs mass resolution. The constraints originate from energy and momentum conservation and from the requirement of one di-jet mass to be $m_Z = 91.187$ GeV. The four momentum of the centre-of-mass system is recalculated after subtraction the four vector of the reconstructed isolated photons from the nominal center-of-mass system.

$$(\vec{p}, E) = (\vec{0}, 2E_{beam}) - \sum_{\gamma} (\vec{p}_\gamma, E_\gamma) \tag{1}$$

3.2.3 Jet-wise flavour tagging

For the identification of the primary and secondary vertices, a tool developed by the SLD collaboration, ZVTOP [10], is used. Track parameters are used to define a probability density tube for every track. The local probability density is obtained by multiplying the densities of all tracks. Seed vertices are maxima in this combined probability density. Then it is tried to add iteratively additional tracks to the vertex using a χ^2 method. In the last step, tracks belonging to more than 1 vertex are assigned to the vertex closest to the primary vertex.

After this vertex reconstruction, the jets are subdivided into three subsamples:

- only the primary vertex was found;
- one secondary vertex was found;
- more than one secondary vertex was found.

For each of those subsamples, two artificial neural networks (ANNs) [11] are trained to separate the different flavours:

- One ANN (b-net) is trained to identify b-jets. The signal training sample consists of b-jets while the background consists of a mixture of c-jets and gluon jets..
- A second ANN (c-net) is dedicated for the tagging of c-jets. Here, the signal training sample are c-jets and the background consists of b-jets and gluon jets.

200000 jets of each HZ decay channel, HZ $\rightarrow b\overline{b}$, HZ $\rightarrow c\overline{c}$ and HZ $\rightarrow$gg, were used to train the ANNs.

The input variables are the same for b-net and c-net. In the case, that only the primary vertex is found, the tracks are sorted by the impact parameter significance in $\mathrm{r}-\phi$, which is defined as the impact parameter divided by its error. The following input variables are used:

- the impact parameter significance in $\mathrm{r}-\phi$ of the most significant track;
- the impact parameter significance in $\mathrm{r}-\phi$ of the second most significant track;
- the impact parameter significance in z of the most significant track;
- the impact parameter significance in z of the second most significant track;
- the momentum of the most significant track;
- the momentum of the second most significant track;
- the joint probability in $\mathrm{r}-\phi$. The joint probability is an estimator for the probability that all tracks in a jet belong to the primary vertex;
- the joint probability in z;

In the case that at least one additional secondary vertex is found, a different set of input variables is used, including information on the vertex:

- the decay length significance of the secondary vertex, which is defined as the decay length divided by its error;
- the decay length of the secondary vertex;
- the momentum of the secondary vertex, i.e. the sum of the momenta of all tracks associated to the vertex;
- the p_t-corrected mass of the secondary vertex; the momentum of the reconstructed b is corrected for energy probably carried by neutral hadrons and neutrinos. The b flight direction is estimated using the vector from the primary vertex to the secondary vertex. Afterwards, p_t, the momentum of the decay products perpendicular to the b flight direction calculated and -p_t added to the vertex momentum vector and the invariant vertex mass is calculated using this corrected vertex momentum;
- the track multiplicity of the secondary vertex;
- the vertex probability calculated from the χ^2 of the vertex;
- the joint probability in $\mathrm{r}-\phi$;
- the joint probability in z.

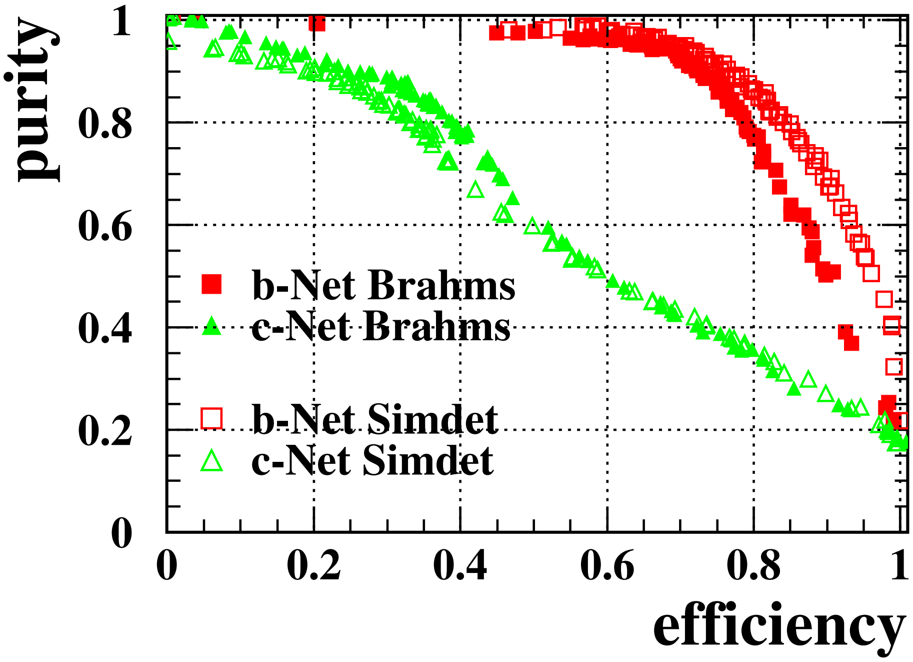

Figure 1: *Comparison of the flavour tagging performance for BRAHMS (closed symbols) and SIMDET (open symbols). The triangles show the efficiency vs. purity using different cuts for the charm tag (c-net) and the squares for the bottom tag (b-net).*

Figure 1 shows the comparison between SIMDET and BRAHMS events generated with the same detector configuration for which the track parameter parametrisation for SIMDET was extracted. It shows the purity of the selected sample as a function of the signal efficiency for the b-net and the c-net. The events are $q\overline{q}$ events simulated at a centre-of-mass energy of $\sqrt{s} = 91.2\,\mathrm{GeV}$. The events were forced into two jets and no acceptance cut is applied. The comparison between the fast parametric and the full simulation is very good for the c-net. Also a reasonable agreement between for the b-net is achieved. The difference at very high efficiencies occurs, because of missing resolution tails in the SIMDET simulation.

4 Event selection

In this section, the selection of the signal events is described. This selection is done in three steps. First, all events are divided into three selection channels depending on the Z decay products. Then, for each of these selection channels a cut based selection is applied to reduce the background which is very different from the signal. The third step consists of a likelihood selection to reduce the background further. Events which survive the likelihood selection are used for the branching ratio extraction described in Section 5.

4.1 Channel classification

The topology of the signal does not depend strongly on the Higgs boson decay channel. The first selection step is a classification of the events depending on the decay products of the Z boson into hadrons, leptons or neutrinos. The three classes are defined as follows:

- Leptonic events: Two electrons or two muons, each with at least 15 GeV momentum are required.

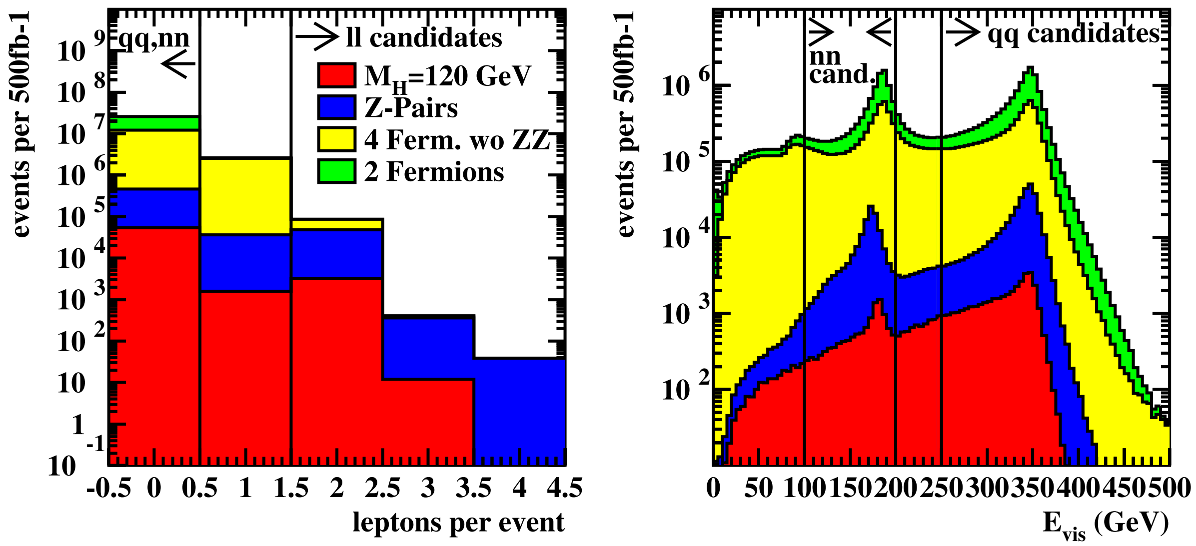

Figure 2: *Distribution of the number of reconstructed leptons per event (left) and visible energy (right) used for the classification of the events in the different selection channels. The black lines and the arrows indicate the acceptance regions for lepton events (ll), hadronic events (qq) and neutrino events (nn).*

- Hadronic events: No lepton and at least 250 GeV of visible energy after photon rejection are required.
- Neutrino events: No leptons and more than 100 GeV and less than 200 GeV of visible energy after photon rejection are required.

Figure 2 shows the distribution of the number of leptons (left) and for the visible energy (right) for Higgs events (red), two-fermion background (green), four-fermion background without Z-Pairs (yellow), and for Z-Pairs (blue).

Table 3 and Table 4 show the total number of expected events in the different selection classes for background and Higgs-strahlung events for various decay modes (signal and background). Approximately 25% of the background events do not satisfy either of the three criteria and are rejected. The latter are mainly events with one detected lepton in the final state ($\mathrm{W^+W^-} \rightarrow \mathrm{qql}\nu$) and events with more missing energy than 100 GeV (radiative returns and single-W and single-Z), where the photons or leptons disappear undetected along the beam pipe. Also 8% of the signal events are rejected at this step. These are mainly events with hadronic τ decays and events with jets close to the beam pipe. This fraction of rejected events for $\mathrm{H} \rightarrow \mathrm{b\bar{b}}$ and $\mathrm{H} \rightarrow \mathrm{c\bar{c}}$ is slightly higher than for $H \rightarrow$gg because of the additional missing energy and additional leptons from semi-leptonic heavy flavour decays.

4.2 The hadronic channel $\mathrm{ZH} \rightarrow \mathrm{q\bar{q}H}$

In the hadronic channel, the Z boson as well as the Higgs boson is decaying into two partons, either quarks or gluons. These partons are fragmented into hadrons. The reconstructed signal consists of four jets. Two of the jets have an invariant mass consistent with m_{Z} and two have a mass consistent with m_{H}. The main background are 2-fermion processes without initial state radiation and badly reconstructed fully hadronic $\mathrm{W^+W^-}$ and $\mathrm{Z^0Z^0}$ events where one boson is not well measured or a hard initial state photon is not tagged correctly.

classif.	2 fermions	W$^+$W$^-$		Z^{0}Z^0			single W and Z	
	qq	qqqq	q$\bar{\mathrm{q}}l\nu$	qqqq	qql$^+$l$^-$	q$\bar{\mathrm{q}}\nu\nu$	qqlν	qqee
all	13635941	3060000	2925000	240000	100000	120000	1236000	6664000
hadronic	7520724	2949753	573834	229746	17616	384	30153	826492
leptonic	22	6	1327	2	44104	0	29	34634
neutrino	4759313	8808	267606	1311	3350	110856	736670	3057748
rejected	1355882	101432	2082232	8941	34929	8759	469146	2745124

Table 3: *Expected number of background events for the different selection channels for an integrated luminosity of* $500\,\mathrm{fb}^{-1}$.

		signal			background			
classification	total H	b$\bar{\mathrm{b}}$	c$\bar{\mathrm{c}}$	gg	W$^+$W$^-$	$\tau^+\tau^-$	Z^{0}Z^0	fusion
all	88864	50813	2266	5002	10027	5025	1097	14633
hadronic	46705	35291	1589	3523	4450	1331	515	7
leptonic	4879	2805	126	271	919	528	132	99
neutrino	25928	9717	430	953	1335	602	224	12667
rejected	11350	3001	122	254	3322	2564	227	1860

Table 4: *Expected Higgs boson events for* $m_H = 120\,\mathrm{GeV}$ *and* $500\,\mathrm{fb}^{-1}$ *for various Higgs decay modes. Also shown is the expected number of events from the WW- and ZZ-fusion processes.*

The selection consists of two parts. First a cut-based selection is applied to reduce the background clearly distinguishable from the signal process. Then a likelihood selection provides a further background suppression.

4.2.1 Cut-based selection

The following cuts are applied to reject events which do not look signal-like:

1 $\mathrm{n_{tracks}} > 13$: signal events are required to have more than 13 reconstructed charged particle tracks. This cut rejects purely leptonic background completely.

2 $E_\gamma < 100\,\mathrm{GeV}$: No photon with more than 100 GeV should be reconstructed to reject events with high energetic initial state photons. These hard photons rarely occur in the signal.

3 $|\cos\theta_{\mathrm{thrust}}| < 0.85$: The absolute value of the cosine of the thrust axis has to be less than 0.85. Most of the background processes have a strongly forward peaking angular distribution while Higgs-strahlung events are produced more centrally in the detector.

4 *thrust* < 0.87: The thrust value has to be less than 0.87; Signal events are much less boosted and much more spherical than the background.

5 $log_{10}(y_{34}) > -6.$: y_{34} is the DURHAM resolution parameter, at which the event changes from a four-jet to a three-jet configuration. This cut rejects mostly 2-fermion background.

Figure 3 shows the distribution for the different variables. The cuts are displayed as solid line and the arrow shows the side of the cut which is accepted.

Table 5 and Table 6 show the accepted number of events after each cut for background and signal, respectively. While the background is rejected by a factor of 100, the signal efficiency is 67.7 %.

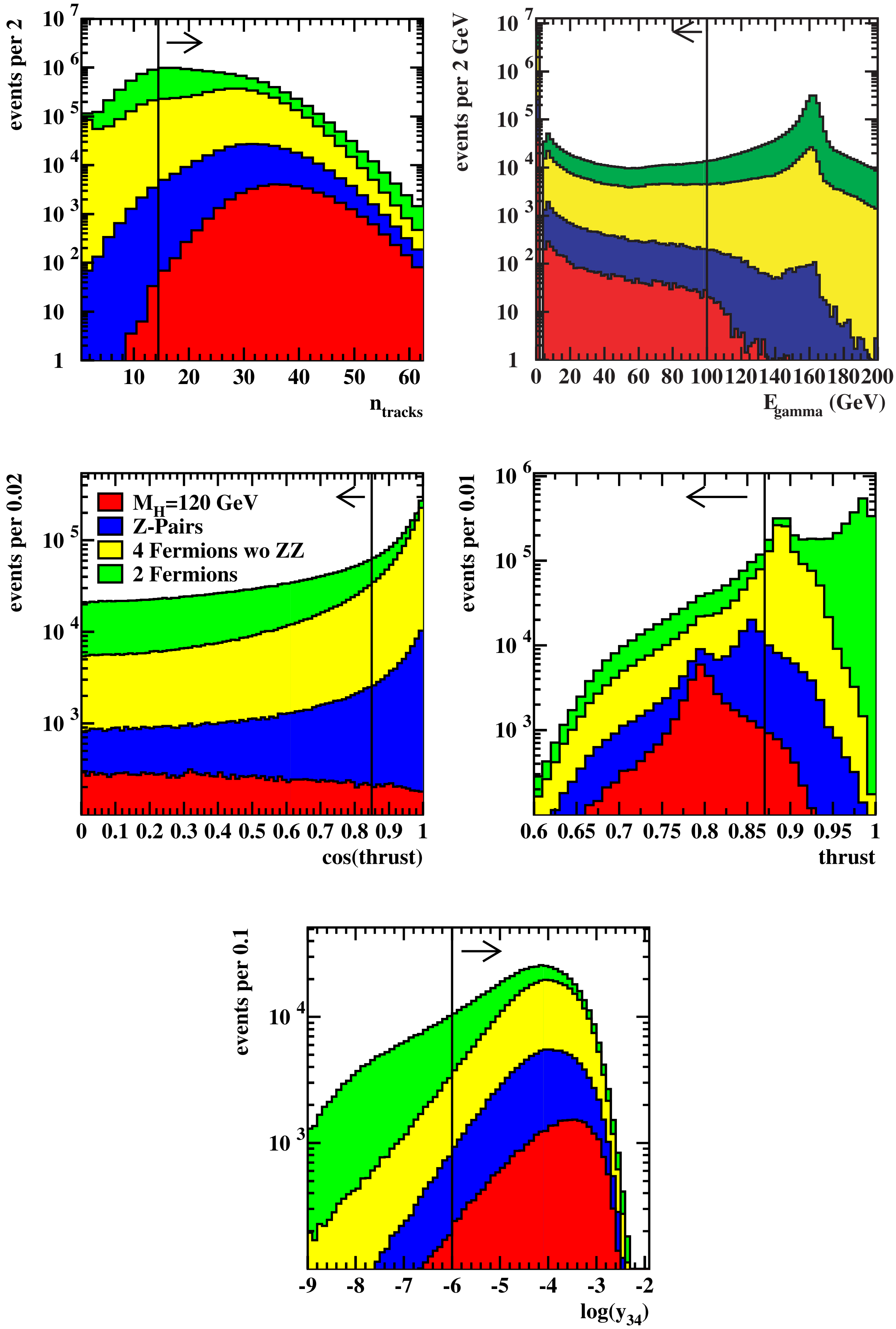

Figure 3: *Variables used for the cut selection in the hadronic channel.*

cut #	total SM background	2 fermions qq	W^+W^- qqqq	qqlν	Z^0Z^0 qqqq	qqll	qq$\nu\nu$	single W and Z qqlν	qqee
0	12148704	7520724	2949753	573834	229746	17616	384	30153	826492
1	9672034	5728573	2936260	372939	227638	13842	278	16422	376080
2	7026330	3437302	2909670	322027	225579	12672	148	3760	115168
3	4098432	2667099	1201293	101970	115994	6161	95	466	5351
4	688393	299192	297077	8947	77945	2908	17	297	2007
5	534357	175643	278412	3380	73843	2443	8	65	560
lh	7621	2569	3799	9	1213	26	0	0	3

Table 5: *Cut flow table for the background processes in the hadronic channel. The first line (0) indicates the events in this selection class, (1) to (5) are the events after cut number (1) to (5), and (lh) shows the events surviving the likelihood selection for* $500\,\mathrm{fb}^{-1}$ *at* $\sqrt{s} = 350\,\mathrm{GeV}$.

cut #	total H	signal $b\bar{b}$	$c\bar{c}$	gg	background W^+W^-	$\tau^+\tau^-$	Z^0Z^0	fusion
0	46705	35290	1589	3523	4449	1331	514	7
1	46508	35272	1586	3523	4439	1165	514	6
2	46340	35154	1580	3512	4422	1156	512	2
3	40852	30998	1391	3087	3888	1034	450	1
4	37141	28117	1260	2888	3638	814	420	1
5	35333	26672	1193	2787	3561	710	407	0
lh	10189	8143	379	771	652	165	78	0

Table 6: *Cut flow table for the different Higgs decay modes in the hadronic channel. The first line (0) indicates the events in this selection class, (1) to (5) the events after cut number (1) to (5), and (lh) the events surviving the likelihood selection for* $500\,\mathrm{fb}^{-1}$ *at* $\sqrt{s} = 350\,\mathrm{GeV}$.

4.2.2 Likelihood selection

To further suppress the remaining background, a likelihood selection with 5 variables and 3 reference classes is applied. Some of the variables are already used in the cut selection. The variables are:

A E_{vis}: the visible energy in the event;

B $log_{10}(y_{34})$: the logarithm of the DURHAM y_{34};

C thrust: the thrust value;

D m_H: the reconstructed Higgs mass of the best 5C-Fit; the best fit is defined as the fit for the jet pairing which yields the smallest χ^2;

E $\cos\theta_{\mathrm{thrust}}$: the direction of the thrust axis, the jet charge is used to estimate the sign of the thrust axis. This additional information helps to reduce W^+W^- background.

For the likelihood calculation, three reference distributions are used:

- Signal events, in which the Z is decaying hadronically;
- Hadronic two-fermion background;
- Fully hadronic four-fermion background from W^+W^- production.

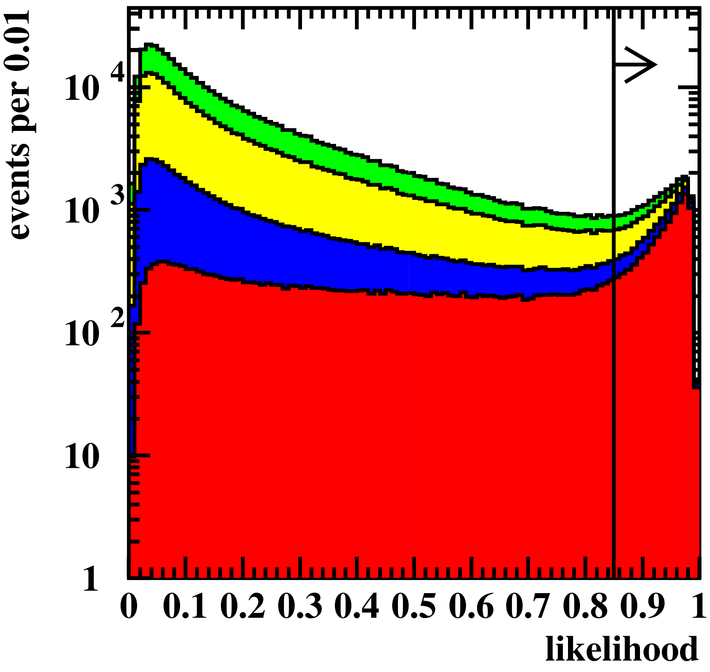

Figure 4: *The likelihood distribution in the hadronic channel.*

It was checked that the inclusion of Z^0Z^0 events into the reference distributions would reduce the separation power of the likelihood, because most of their properties are between those of W-pairs and signal events.

Figure 4 shows the distribution of the likelihood variables. The last lines of Table 5 and Table 6 show the expected number of events for the background and the different Higgs decay channels after the cut on the likelihood $\mathcal{L} > 0.7$. The background is reduced by an additional factor of 500. Also the signal is reduced by factor 3.5. Because of the huge background only signal events which are very well reconstructed are selected. For this reason, the $\mathrm{H} \to \mathrm{b\bar{b}}$ events show a slightly lower selection efficiency than $\mathrm{H} \to gg$ events. Because of the missing energy induced by neutrinos from semileptonic b-decay, the mass resolution for this channel is slightly worse than the mass resolution for Higgs bosons decaying into gluons. This has been taken into account for the extraction of the branching ratios. While it is very important to select as many events in the gluon and charm decay channel as possible, the expected error on the branching ratio into bottom quarks should be by far the smallest because of the large expected branching ratio. A more flavour-independent selection would result in a significant worse signal-to-background ratio.

4.3 The leptonic channel $\mathrm{ZH} \to \ell^+\ell^- \mathrm{H}$

In the leptonic channel, the final state consists of two leptons from the Z and two hadronic jets from the Higgs boson. Because of the powerful lepton identification and the very good single-track resolution of the ILC detectors, the most important background also consists of two leptons coming from a Z recoiling against a hadronic system with a large invariant mass, in particular Z-pairs and single-Z production. Again a two step selection, i.e. a cut and a likelihood selection, is applied.

4.3.1 Cut-based selection

The preselection cuts are optimised for the selection of the two leptons with an invariant mass consistent with m_Z recoiling against two jets with a large invariant mass:

1 $n_{leptons} \geq 2$: two or more leptons, where at least two are required to have the same flavour. This cut rejects purely hadronic background completely and the semileptonic W-pairs by a large amount;

2 $70\,\text{GeV} < m_{ll} < 110\,\text{GeV}$: the invariant mass of the two lepton system has to between 70 and 110 GeV. After this cut, the background with two leptons not coming from a Z-boson decay is rejected nearly completely;

3 $m_{jj} > 100\,\text{GeV}$ and $|\cos\theta_{\text{thrust}}| < 0.9$: two jets with an invariant mass larger than 100 GeV are required and the cosine of the thrust axis has to be smaller then 0.9. These two cuts reject a large part of the Z-pair background and only a small fraction of the single-Z events are surviving.

After these three cuts, the background sample consists mainly of Z-Pairs and a small fraction of single-Z events. Figure 5 (left) shows the distribution of the invariant di-lepton mass. The numbers of events after the different cuts are shown in Table 7 and Table 8 for background and signal, respectively. While the cut based selection in the $q\bar{q}$ channel yields a high background reduction, in the leptonic channel the cut based selection reduces the background from Z-pairs only by a factor of 20 and while retaining about 67

	total SM	2 fermions	W^+W^-		Z^0Z^0			single W and Z	
	background	qq	qqqq	qqlnu	qqqq	qqll	qqnn	qqlnu	qqee
0	80125	22	6	1327	2	44104	0	30	34634
1	78447	14	5	652	1	43602	0	18	34154
2	45767	2	2	319	0	30873	0	3	14567
3	2908	0	1	7	0	2699	0	0	201
lh	676	0	0	2	0	625	0	0	49

Table 7: *Cut flow for the background in the leptonic channel. (0) indicates the number of events after the channel classification while (1)-(3) are the different precuts. The last line (lh) summarises the number of events after the likelihood selection.*

		signal			background			
	total H	$b\bar{b}$	$c\bar{c}$	gg	W^+W^-	$\tau^+\tau^-$	Z^0Z^0	fusion
0	4879	2804	125	271	919	528	131	98
1	4494	2764	124	268	738	409	129	59
2	3834	2565	115	251	516	283	89	12
3	2389	1846	89	201	207	20	27	0
lh	1915	1467	73	173	170	12	21	0

Table 8: *Cut flow for the Higgs decay modes in the leptonic channel. (0) indicates the number of events after the channel classification while (1)-(3) are the different precuts. The last line (lh) summarises the number of events after the likelihood selection.*

4.3.2 Likelihood selection

The likelihood selection is used to reduce the main background process, consisting of Z^0Z^0 events. The variables are sensitive to the measured Higgs mass and the angular distribution of the jets:

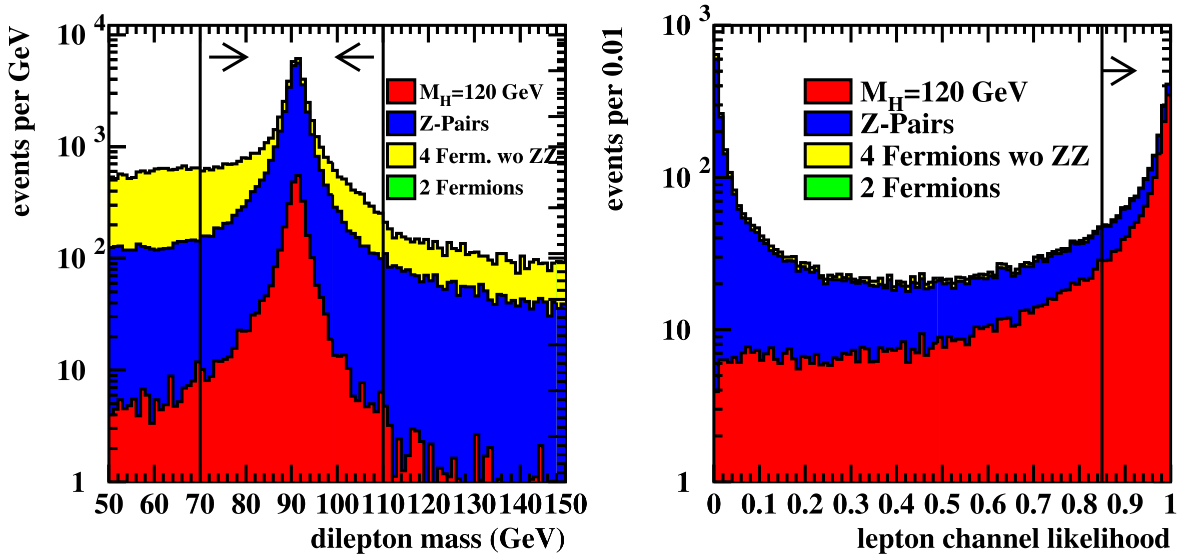

Figure 5: *Distribution of the invariant two lepton mass (left) and the likelihood distribution (right) for the leptonic channel. The vertical lines with the arrows indicate the region accepted by the analysis.*

A $|\cos\theta_{\text{thrust}}|$, the absolute value of the cosine of the thrust axis. The background is peaking in the forward direction while the signal is produced more central;

B Thrust: the invariant mass of the Higgs boson is larger than the one of the Z. Because of this, a more spherical distribution of the decay products is expected.

C m_{jj}^{5C}: the invariant mass of the two hadronic jets using the kinematic Fit (5C). This is mainly to reduce Z-pairs;

D m_{jj}^{raw}: the invariant mass of the two hadronic jets using the raw jet momenta.

E $|E_{jet1} - E_{jet2}|$: The difference of the two energies of the hadronic jets. Because of the larger boost in events from Z-pair production, it is expected to observe a larger jet energy spread than in signal events.

Two reference classes are used:

- Signal
- Z-pairs, where one Z boson is decaying leptonically and one hadronically.

Figure 5 (right) shows the distribution of the likelihood and the last lines of Table 7 and Table 8 show the number of expected events after likelihood selection for background and the different Higgs decay channels. The likelihood selection reduces the remaining background by a factor of 5 while the overall signal efficiency is around 44%.

The leptonic channel has the largest signal efficiency of all channels and the largest signal-to-background ratio. However, because of the small branching ratio of the Z boson into electrons and muons, this channel has by far the smallest sensitivity.

4.4 The neutrino channel $\mathrm{ZH} \rightarrow \nu\overline{\nu}\,\mathrm{H}$

The selection for the neutrino channel is the most difficult. The signal topology consists of two hadronic jets from the Higgs Boson recoiling against two neutrinos from the Z boson decay. The reconstructed invariant mass of the hadronic system is expected to be consistent with the Higgs mass and the recoil mass should be consistent with m_{Z}. The background consists of 2-fermion events with undetected photons from ISR, semileptonic W-Pairs where the lepton disappears along the beam line, Z-Pairs decaying to hadrons and neutrinos and single $\mathrm{W}^{\pm}$ and Z production where the leptons are scattered under a low angle w.r.t. the beam pipe.

4.4.1 Cut based selection

In the channel definition already a moderate visible energy between 100 and 200 GeV is required and no reconstructed high energetic isolated lepton is allowed. For the further selection cuts, mainly angular distributions and mass information are used to reduce the background. The following cuts are applied:

1 $n_{\mathrm{tracks}} > 10$: More than 10 charged particle tracks in the event are required to reject purely leptonic events;

2 $E_{\gamma} < 100\,\mathrm{GeV}$: Less than 100 GeV of energy associated with identified photons are required to reject 2-fermion radiative return events;

3 $|\cos\theta_{\mathrm{sphericity}}| < 0.9$: The absolute value of the cosine of the polar angle of the sphericity axis should be smaller than 0.9;

4 $|cos\theta_{\mathrm{thrust}}| < 0.98$: The cosine of the polar angle of the thrust axis should be smaller than 0.98. The thrust axis is much less well defined in this channel than for the hadronic or leptonic events. Nevertheless it has some remaining discriminating power;

5 $100\,\mathrm{GeV} < m_{jj} < 140\,\mathrm{GeV}$: the event is forced into two jets using the DURHAM algorithm, The dijet mass should be larger than 100 GeV and smaller than 140 GeV to reject low invariant mass hadronic systems from W-airs, Z-pairs and and two-photon events.

6 $|\cos\theta_{\mathrm{miss}}| < 0.65$: The missing energy vector should not point into the forward region of the detector.

Figure 6 shows the distribution of the variables used for the cut-based selection in the neutrino channel. Table 9 and Table 10 show the expected numbers of events after each cut. After the selection, the background is reduced by a factor 1000.

4.4.2 Likelihood selection

After the cut selection a likelihood selection is performed using the following variable:

A the visible energy;

B the absolute value of the cosine of the thrust axis polar angle;

C the thrust value;

D the angle between the two jets;

E the di-jet mass;

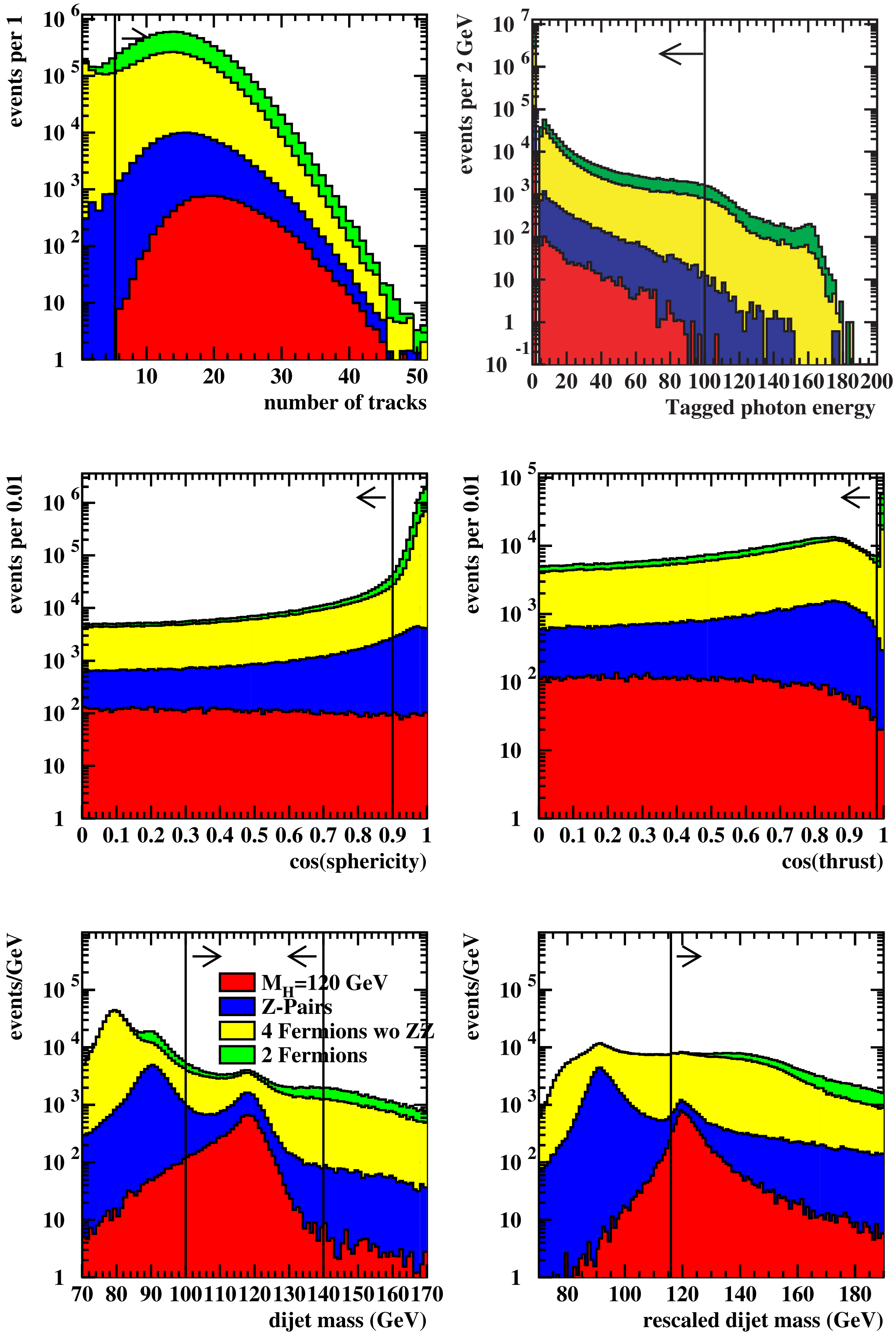

Figure 6: *Variables used for the cut-based selection in the neutrino channel.*

F The rescaled di-jet mass $(m_{jj})_{\text{rescaled}}$. The jet energies are rescaled with the assumption, that they are produced in a Z^0 decay:

$$(m_{jj})_{rescaled} = m_{jj} \times x_{\text{rescal}} \tag{2}$$

with

$$x_{\text{rescal}} = \frac{\sqrt{s} \times (E_{jet1} + E_{jet2})}{m_{jj}^2} - \sqrt{\left(\frac{\sqrt{s} * (E_{jet1} + E_{jet2})}{m_{jj}^2}\right)^2 - \frac{s - m_Z{}^2}{m_{jj}^2}} \tag{3}$$

$\sqrt{s}$ is the nominal center-of-mass energy while E_{jet} are the measured jet energies.

G The cosine of the polar angle of the sphericity axis.

Reference distributions are constructed for the following classes:

- signal where the Z-boson is decaying into two neutrinos;
- hadronic two-fermion background;
- Z-pairs where one Z-bosons is decaying hadronically and the other one into two neutrinos.

	total SM background	2 fermions	W^+W^-		Z^0Z^0			single W and Z	
		qq	qqqq	qqlnu	qqqq	qqll	qqnn	qqlnu	qqee
0	8945664	4759313	8808	267606	1311	3350	110856	736670	3057749
1	6657392	3798791	8709	238587	1145	2806	99125	643745	1864484
2	6641823	3790511	8701	238265	1144	2803	99045	639475	1861880
3	833293	155323	3373	134955	312	1371	66264	433909	37785
4	769775	113361	3271	134055	281	1339	65707	428818	22943
5	101263	22471	429	58748	43	607	6126	7388	5449
6	78903	14480	409	49400	35	524	4687	6158	3210
lh	1602	11	0	725	0	8	589	270	0

Table 9: *Cut flow table for the SM background in the neutrino channel. (0) indicates-the events after class selection (1)-(6) after the selection cuts and (lh) after the final likelihood selection.*

		signal			background			
	total H	$b\overline{b}$	$c\overline{c}$	gg	W^+W^-	$\tau^+\tau^-$	Z^0Z^0	fusion
0	25928	9717	429	953	1335	601	223	12667
1	25004	9623	418	952	1279	221	215	12294
2	25002	9622	418	952	1278	221	215	12293
3	22358	8836	386	874	1169	198	197	10696
4	22246	8801	385	871	1166	197	196	10628
5	19186	7498	362	851	863	85	113	9415
6	18385	7117	345	810	829	83	108	9093
lh	5029	3756	191	411	255	5	34	377

Table 10: *Cutflow table for the different Higgs decay channels in the neutrino channel. (0) indicates the events after selection cuts (1)-(6) after and after the final likelihood selection (lh).*

Figure 7 shows the final likelihood distribution. The results after the likelihood cut are displayed in Table 9 for background and in Table 10 for the different Higgs decay channels. In the end the signal-to-background ratio is close to the one achieved in the leptonic channel at a signal efficiency of around 37%. The bigger branching fraction and the complementarity of the neutrino channel to the hadronic channel in the background composition make this channel very important for the branching ratio extraction.

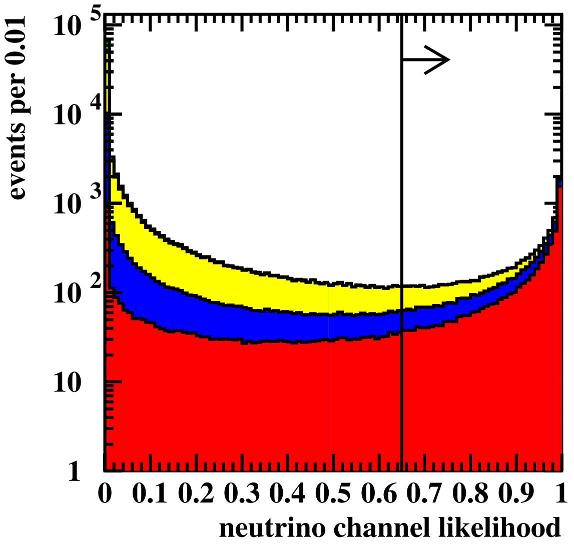

Figure 7: *Likelihood distribution in the neutrino channel.*

5 Branching ratio extraction

The last step of the analysis is the statistical extraction of the flavour content of the selected Higgs candidate events. This leads directly to the branching fraction of the Higgs bosons because gluon splitting into charm and bottom quarks is small compared to the expected errors. The fraction of Higgs signal events originating from $\mathrm{H} \rightarrow \mathrm{b\bar{b}}, \mathrm{c\bar{c}}, gg$ is extracted from a simultaneous fit of two event-wise tagging variables, the b-likeness and c-likeness which are sensitive to the bottom and charm content of an event, respectively.

Table 11 summarises the numbers of events which are subjected to the branching ratio analysis for the three selection channels. Table 12 details the true flavour composition of these events as well as the selection efficiency for each Higgs decay mode separately. The difference in the selection efficiencies for different Higgs decay modes is taken into account in the branching ratio fit.

selection	total	signal	Higgsbg	bg
qqqq	17810	9294	895	7621
qqll	2591	1712	203	676
qq$\nu\nu$	6631	4358	671	1602
all	27032	15394	1769	9899

Table 11: *Final numbers of events in the three selection channels entering the branching ratio fit.*

5.1 Fit procedure

A cut based separation of the flavour channels with a high selection efficiency and purity does not yield the highest possible sensitivity. As an example, for the $\mathrm{H} \rightarrow \mathrm{c\bar{c}}$ decay, the background from $\mathrm{H} \rightarrow \mathrm{b\bar{b}}$, as well as from $\mathrm{H} \rightarrow gg$ is of the same order as the expected number of signal events. To yield the best sensitivity, a binned maximum likelihood method was used to extract the hadronic Higgs branching ratios. The two-dimensional distribution of b-likeness vs. c-likeness expected for the three hadronic Higgs decay modes under consideration as well as the expected

decay mode	selected events qq	ll	nn	selection efficiency qq	ll	nn
$b\bar{b}$	8143	1467	3756	16.02	2.89	7.39
$c\bar{c}$	379	73	191	16.72	3.22	8.42
gg	771	173	411	15.41	3.46	8.22
W^+W^-	652	170	255	6.50	1.69	2.54
$\tau^+\tau^-$	165	12	5	3.28	0.24	0.68
Z^0Z^0	78	21	34	7.11	1.91	3.10
fus		0	377	—	—	2.58

Table 12: *Numbers of selected events and selection efficiencies in the three channels for each Higgs decay mode separately.*

background distribution were fitted to the simulated data distribution, keeping the shapes fixed and allowing the normalisation of each contribution to vary. The method takes care of the correlation between the three selection channels selection and the different decay modes as well as the background.

For each event the b-likeness and c-likeness was calculated from jet flavour tagging neural net values of the two jets supposed to originate from the Higgs decay. The b/c-likeness are calculated as

$$X - likeness = \frac{X_1 \cdot X_2}{X_1 \cdot X_2 + (1 - X_1) \cdot (1 - X_2)} \tag{4}$$

where $X = b$ or c. X_1 and X_2 are the b/c-tag neural net outputs of the first and second jet, respectively.

For each of the three selection channels, four reference distributions were produced: one for each of the hadronic Higgs decay modes (bottom, charm an gluons), using a pure sample and applying the full selection chain. The fourth reference distribution includes the SM background as well as the non-hadronic Higgs decay modes. The branching fraction of the Higgs Boson into non hadronic modes and the SM background expectation are fixed.

While it is well justified to consider the SM background expectation to be known (within small systematic errors) fixing the non-hadronic Higgs decays in the fit may lead to a biased measurement. There are at least two viable solutions to this problem.

The first solution, which we explore here, uses the fact that the dominant non-hadronic Higgs decays which can pollute the hadronic sample are $H \to W^+W^-$ and $H \to ZZ$ as well as $H \to \tau^+\tau^-$. All of these Higgs decays rates can be measured separately with negligible cross contamination from hadronic Higgs decays using final state leptons (see e.g. [15]) which allow to assume them known in this analysis.

The following likelihood function is used in the fit:

$$-2\log L(r_{bb}, r_{cc}, r_{gg}) = \sum_{i=1}^{n_{ch}} \sum_{j=1}^{n_b} \sum_{k=1}^{n_c} \frac{\left(N_{ijk}^{data} - \sum_{s=(bb,cc,gg,bkg)} r_s N_{ijk}^s\right)^2}{N_{ijk}^{data}} \tag{5}$$

The fit parameters r_{bb}, r_{cc}, r_{gg} are the the numbers of expected events from the three hadronic Higgs decays divided by the corresponding numbers of events for SM-Higgs branching ratios. The relative background rate r_{bkg} is set to 1 as explained above. N_{ijk}^s are the number of expected events in each bin (j, k) of the two-dimensional b-likeness vs. c-likeness distribution in selection channel (hadronic, lepton, neutrino) i. The numbers are obtained from distributions which correspond to approximately ten times the assumed data luminosity of 500 fb^{-1} in order to suppress statistical fluctuations to a tolerable level. N_{ijk}^{data} is the number of simulated (fake) data events in each bin.

The measured quantities, cross sections times branching ratio, are calculated from the fitted parameters r_s according to:

$$\sigma(e^+e^- \to \mathrm{HZ}) \times \mathrm{BR}(\mathrm{H} \to s) = r_s \times BR(\mathrm{H} \to s)_{SM} \times \sigma(e^+e^- \to \mathrm{HZ})_{SM} \tag{6}$$

In order to obtain absolute Higgs branching ratios, these measured quantities have to be divided by the measured total cross section for Higgs-strahlung obtainable from the recoil mass distribution independent from the Higgs branching ratios.

5.2 Results

In Fig. 8 the c-likeness vs b-likeness distribution is shown for H $\to \mathrm{b\overline{b}}$, H $\to \mathrm{c\overline{c}}$, H $\to$ gg and for the SModel background including remaining non-hadronic Higgs decays.

For the measurement of the topological cross sections $\sigma(e^+e^- \to \mathrm{HZ}) \times \mathrm{BR}(\mathrm{H} \to s)$ (normalized to the SM Higgs-strahlung total cross section σ_{SM}, in order to obtain units of branching ratios) we obtain the following projected results:

$$(\sigma BR(H \to b\bar{b}))/\sigma_{SM} = 68.16 \pm 0.67\% \tag{7}$$
$$(\sigma BR(H \to c\bar{c}))/\sigma_{SM} = 3.04 \pm 0.37\% \tag{8}$$
$$(\sigma BR(H \to gg))/\sigma_{SM} = 6.71 \pm 0.43\% \tag{9}$$

The corresponding relative errors are

$$\frac{\Delta\sigma BR}{\sigma BR}(H \to b\bar{b}) = 1.0\% \tag{10}$$
$$\frac{\Delta\sigma BR}{\sigma BR}(H \to c\bar{c}) = 12.3\% \tag{11}$$
$$\frac{\Delta\sigma BR}{\sigma BR}(H \to gg) = 8.3\% \tag{12}$$

5.3 Systematic errors and detector performance

We do not aim at performing a full investigation of experimental systematics in this study. It is obvious that a very good understanding of the detector performance and response is needed. Also, SM backgrounds have to be understood at the percent level. On the other hand it is very likely that this can be achieved with 500 fb^{-1} of data and corresponding precision calculations of SM processes. The uncertainties on $H \to c\bar{c}$ and H $\to gg$ will certainly be statistics limited. To achieve a systematic uncertainty of 1% in the $b\bar{b}$ channel is somewhat more demanding. However, given the manifold possibilities for calibration and cross checks we are convinced this can be achieved.

5.3.1 Fit stability

Here, we study in particular the stability of the obtained expected uncertainties.

The fit was repeated with 10 independent pseudo-data samples to check the obtained errors and estimate the bias of the fitting procedure. In Table 13 the results for the ten independent samples are shown. The variation of the fitted central values nicely agrees with the expectation from the fit errors. No significant bias is observed.

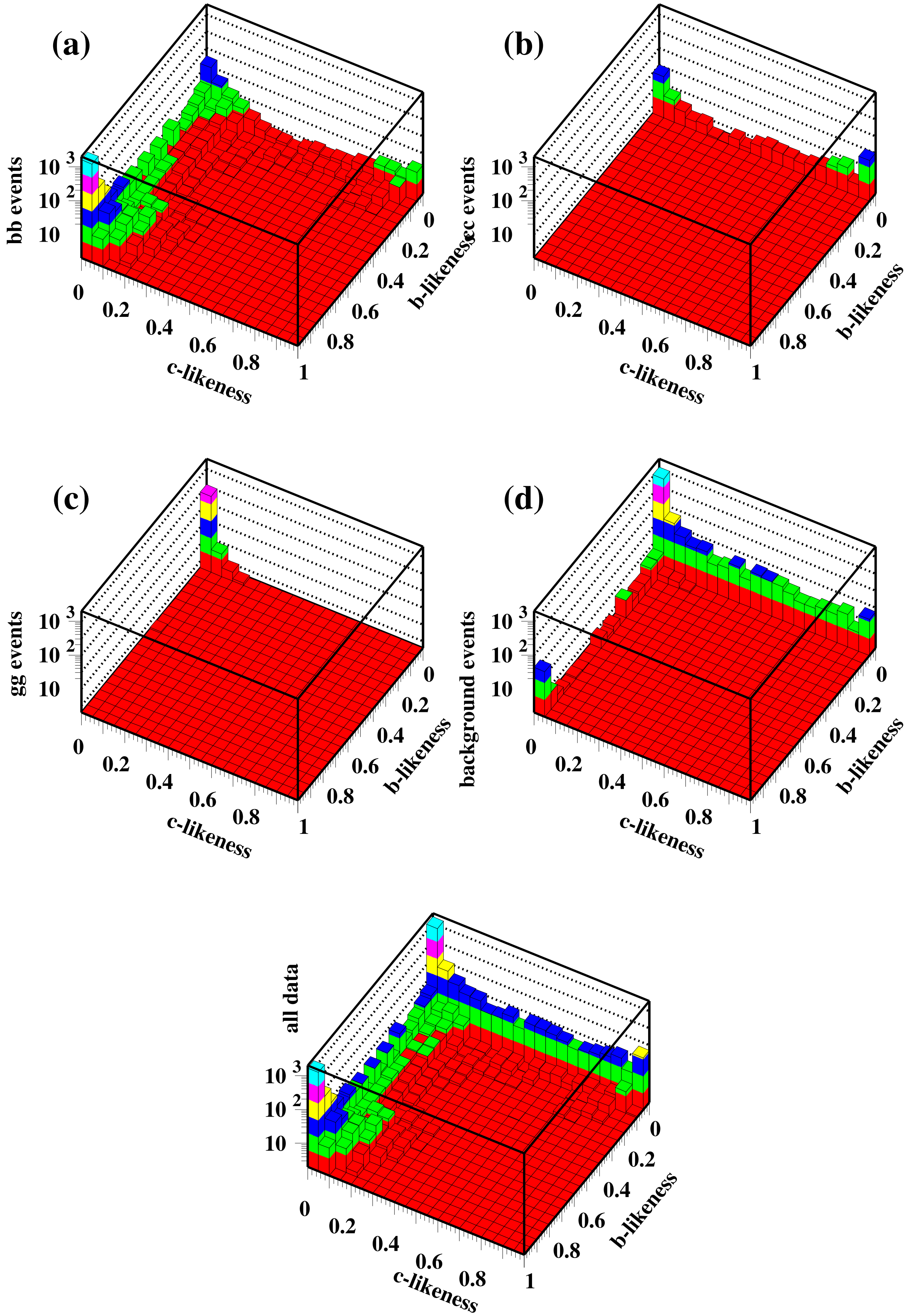

Figure 8: *B- vs C-Likeness distributions for $H \to b\bar{b}$, $H \to c\bar{c}$, $H \to gg$, $H \to b\bar{b}$, SM background and all selected events after final selection in the neutrino channel.*

set of data	hbb	hcc	hgg
1	0.9922+ 0.0098 -0.0097	1.0201+ 0.1218 -0.1191	1.0225+ 0.0836 -0.0829
2	0.9996+ 0.0098 -0.0098	0.8303+ 0.1189 -0.116	0.9398+ 0.0830 -0.0820
3	0.9900+ 0.0098 -0.0097	1.0128+ 0.1217 -0.1190	0.9336+ 0.0828 -0.0823
4	0.9958+ 0.0098 -0.0097	0.9952+ 0.1210 -0.1186	1.0390+ 0.0836 -0.0830
5	0.9978+ 0.0098 -0.0098	1.1514+ 0.1237 -0.1220	0.9686+ 0.0839 -0.0828
6	1.0066+ 0.0098 -0.0098	0.9852+ 0.1205 -0.1183	1.0213+ 0.0834 -0.0826
7	1.0125+ 0.0099 -0.0098	0.9675+ 0.1207 -0.1183	1.0484+ 0.0836 -0.0830
8	1.0051+ 0.0098 -0.0098	1.0528+ 0.1212 -0.1188	0.9778+ 0.0832 -0.0825
9	0.9997+ 0.0098 -0.0098	0.9315+ 0.1217 -0.1189	0.9843+ 0.0829 -0.0824
10	1.0003+ 0.0098 -0.0098	1.0539+ 0.1231 -0.1206	1.0512+ 0.0837 -0.0832

Table 13: *Fit results of different independent samples.*

5.3.2 Fits using only parts of the data

The study was repeated with some of the three selection channels left out in order to obtain insight into the relative importance of the channels.

In Table 14 the results for fits where only two or only one of the three selections were used. It can be seen that different selections channels have different relative importance for the accuracy on the different decay modes. As an example, the accuracy on $\mathrm{H} \to \mathrm{b\bar{b}}$ is is dominated by the hadronic channel, due to its high statistics. On the other hand, the neutrino channel, which has a better purity, yields the largest impact on $\mathrm{H} \to gg$ branching ratio. The different background composition in the different channels provides additional separation power. Therefore, the approach to keep the b- vs. c-distributions separate for the channels during the fit leads to more precise results than what would be obtained if they were simply added together.

5.3.3 Dependence on the silicon vertex detector performance

An interesting question for the vertex detector design is to what extent the achievable precision is depending on the layout of the detector. The study was repeated with a modified vertex detector setup. The track parameter resolutions were recalculated using BRAHMS for a vertex detector omitting the innermost layer and increasing the thickness of the CCD pixel layers from 50 μm to 100 μm [14]. The result is shown in the last line of Table 14. The study shows that these modifications have no significant impact on the precision on $BR(\mathrm{H} \to \mathrm{b\bar{b}})$ branching while the error on $BR(\mathrm{H} \to \mathrm{c\bar{c}})$ increases by approximately 15%.

set of data	hbb	hcc	hgg
1	0.9922+ 0.0098 -0.0097	1.0201+ 0.1218 -0.1191	1.0225+ 0.0836 -0.0829
no neutrinos	0.9892+ 0.0118 -0.0117	1.0097+ 0.1601 -0.1566	1.0961+ 0.1142 -0.1134
no leptons	0.9929+ 0.0104 -0.0104	1.0323+ 0.1323 -0.1294	0.9966+ 0.0931 -0.0925
no hadrons	0.9948+ 0.0151 -0.0150	1.0083+ 0.1616 -0.1566	0.9947+ 0.1028 -0.1017
only leptons	0.9888+ 0.0286 -0.0281	0.9595+ 0.3173 -0.3017	1.1286+ 0.1914 -0.1875
only neutrinos	0.9972+ 0.0179 -0.0177	1.0253+ 0.1890 -0.1823	0.9378+ 0.1224 -0.1207
only hadrons	0.9895+ 0.0130 -0.0129	1.0291+ 0.1867 -0.1823	1.0778+ 0.1432 -0.1422
4 layer SI	1.0048+ 0.0099 -0.0099	1.0155+ 0.1384 -0.1360	1.0052+ 0.0871 -0.0864

Table 14: *Fit results for data set 1 with different combinations of channels switched off and for a modified vertex detector layout (see text).*

6 Measurement of the hadronic branching ratios for a Higgs mass of 140 GeV

The analysis was repeated for a Higgs boson mass of 140 GeV. At this mass the extraction of the signal is more difficult. While the hadronic branching ratios of the Higgs boson drop by a factor of three the branching fraction into WW rises to approximately 50%. Therefore Higgs bosons decaying into WW have to be considered as an additional substantial background.
We try to minimize the differences for the analysis of $m_H = 140\,\text{GeV}$ compared to $m_H = 120\,\text{GeV}$. The same preselection was applied except that all lower mass cuts were raised by 20 GeV. For the likelihood selections the mass windows were also changed accordingly.

6.0.4 WW veto

In order to seperate the H→WW-background from hadronic Higgs boson decays, a dedicated analysis for this Higgs Boson decay channel is in preparation [16]. There, the goal is to add an additional variable which represents the WW-likeness into the branching ratio fit.

In this note, a simplified approach to reject events from HZ→WWZ was used: first, the decay products of the Z were removed from the events. Then all remaining reconstructed particles were forced into 4 jets. Events from HZ→WWZ with W→ hadrons are expected to have a large di-jet masses for all jet combinations. Higgs decays into $b\bar{b}, c\bar{c}, gg$ will always yield some di-jet combinations with low invariant mass. If any of the possible di-jet combinations has an invariant mass below 20 GeV, the event is accepted as signal. Furthermore, if for any of the possible jet-pairings the sum of the two di-jet masses is smaller than 50 GeV, the event is also accepted as signal. All other events are rejected.

6.0.5 Branching ratio fit

Because of the lower signal cross section, a fit for simualted data corresponding to $500\,\text{fb}^1$ occurs to be very unstable. Especially the fitting of the charm branching ratio is very difficult. In addition to the large uncertainty of about 40% the fitted branching ratios are pulled systematically towards very low values.

In order to get a rough estimate of the expected uncertainties, we assume an integrated luminosity of $1000\,\text{fb}^{-1}$. This leads to following results.

$$(\sigma BR(H \to b\bar{b}))/\sigma_{SM} = 34.11 \pm 0.61\% \tag{13}$$
$$(\sigma BR(H \to c\bar{c}))/\sigma_{SM} = 1.52 \pm 0.41\% \tag{14}$$
$$(\sigma BR(H \to gg))/\sigma_{SM} = 4.68 \pm 0.75\% \tag{15}$$

The results shows that a rather precise estimation of the branching ratios for $m_H = 140\text{GeV}$ is possible. For $500\,\text{fb}^{-1}$, the errors for a stable fit should be roughly $30 - 40\%$ larger, however this clearly needs further studies, which include a simultaneous fit of $H \to$ WW.

7 Summary and Discussion.

We describe an analysis for the measurement of the hadronic branching ratios of a Standard Model like Higgs Boson at a centre-of-mass energy of $\sqrt{s} = 350\,\text{GeV}$ and for an integrated luminosity of $500\,\mathrm{fb}^{-1}$ selecting event from the Higgs-strahlung process. The analysis is based on fast detector simulation. However, the most critical part of the analysis, the flavour tagging, exploits a realistic simulaltion using the ZVTOP algorithm with a performance tuned to results obatined from full simulation.

The relative statistical errors obtained for the measurement of $\sigma\times$ BR(H→X) using a simultaneously fit on three selection channels are 1.0% (X= $b\bar{b}$), 12.3% (X= $c\bar{c}$), and 8.3% (X= gg) for $m_H = 120$GeV. The results are compared to previous studies taking the different analyses techniques into account. The results presented in the TESLA TDR [1] yield a 50% smaller error on the production rates for H $\rightarrow c\overline{c}$ and H $\rightarrow$ gg. While the selection procedure is very similar there are differences in the flavour tag. Instead using a track wise vertexing like ZVTOP a jet-wise flavour tag parameterisation was extracted with BRAHMS using well separated jets. This method does not include effects from jet-finding of jets which are close together like the false assignment of tracks. It also does not include merged jets and the jet energy dependence of the estimation.
The results presented at Snowmass 2001 [2] use a similar flavour tag as used in this study. The results for the flavour tag itself have been checked to agree on the level of a few percent. Here difference lies in the selection procedure, which is based on individual cuts rather than on the maximum likelihood method. This leads to bigger errors for the production rates mainly because of the resulting higher impurity of the charm tag. Taking this into account the results are compatible.

References

[1] TESLA Technical Design Report, DESY-2001-011.

[2] C. T. Potter, J. E. Brau and M. Iwasaki, *Standard model Higgs Boson branching ratio measurements at a linear collider* in *Proc. of the APS/DPF/DPB Summer Study on the Future of Particle Physics (Snowmass 2001)* ed. N. Graf, eConf **C010630** (2001) P118.

[3] J-C. Brient,*The direct method to measure the Higgs branching ratios at the future e+ e- linear collider*,LC-PHSM-2002-003

[4] M. Pohl and H. J. Schreiber, *SIMDET - Version 4: A parametric Monte Carlo for a TESLA detector*, arXiv:hep-ex/0206009.

[5] T. Sjostrand, L. Lonnblad and S. Mrenna, *PYTHIA 6.2: Physics and manual*, arXiv:hep-ph/0108264.

[6] T. Ohl, *CIRCE version 1.0: Beam spectra for simulating linear collider physics*, Comp. Phys. Comm. **101** (1997), 269.

[7] P. Janot, *Physics at LEP2*, CERN 96-01, Vol.2, 309.

[8] A. Djouadi, J. Kalinowski and M. Spira, *HDECAY: a Program for Higgs Boson Decays in the Standard Model and its Supersymmetric Extensions*, Comp. Phys. Comm. **108** (1998), 56.

[9] T. Behnke, G. Blair *et al*,*BRAHMS: A Monte Carlo for a Detector at a 500/800 GeV Linear Collider*, LC-TOOL-2001-005

[10] D. Jackson, Nucl. Inst. and Meth. **A388** (1997) 247.

[11] R. Hawkings, *Vertex detector and flavour tagging studies for the TESLA linear collider*, LC-PHSM-2003-021, S.M. Xella-Hansen *et al.*,*Update on flavour tagging studies for the Future Linear Collider using the Brahms simulation*, LC-PHSM-2003-061

[12] K. Desch, T. Klimkovich, T. Kuhl, A. Raspereza,*Study of Higgs Boson Pair Production at Linear Collider*, LC-PHSM-2004-006

[13] Y. Dokshitzer, J.Phys. **G17**, (1991), 1537;
N. Brown, W. J. Stirling, Phys. Lett. **B252** (1990) 657;
S. Bethke et al., Nucl. Phys. **B370** (1992) 310;
S. Catani et al., Phhys. Lett. **B269** (1991),432;
N. Brown, W. J. Stirling, Z. Phys. **C53** (1992) 629.

[14] S. M. Xella Hansen, M. Wing, D. J. Jackson, N. De Groot and C. J. S. Damerell

[15] J.C. Brient, *Measurement of the Higgs decays into WW^* at FLC*, LC-PHSM-2004-002
LC-PHSM-2003-061

[16] J. Samson, PhD thesis in preparation.